

Direct force measurement of the stability of poly(ethylene glycol)–polyethylenimine graft films

Ijeoma M. Nnebe^a, Robert D. Tilton^{a,b}, James W. Schneider^{a,*}

^a Department of Chemical Engineering, Carnegie Mellon University, Pittsburgh, PA 15213-3890, USA

^b Department of Biomedical Engineering, Carnegie Mellon University, Pittsburgh, PA 15213-3890, USA

Received 29 December 2003; accepted 19 March 2004

Available online 6 May 2004

Abstract

The stability and passivity of poly(ethylene glycol)–polyethylenimine (PEG–PEI) graft films are important for their use as antifouling coatings in a variety of biotechnology applications. We have used AFM colloidal-probe force measurements combined with optical reflectometry to characterize the surface properties and stability of PEI and dense PEG–PEI graft films on silica. Initial contact between bare silica probes and PEI-modified surfaces yields force curves that exhibit a long-range electrostatic repulsion and short-range attraction between the surfaces, indicating spontaneous desorption of PEI in the aqueous medium. Further transfer of PEI molecules to the probe occurs with subsequent application of forces between $FR = 300$ and $500 \mu\text{N/m}$. The presence of PEG reduces the adhesive properties of the PEI surface and prevents transfer of PEI molecules to the probe with continuous contact, though an initial desorption of PEI still occurs. Glutaraldehyde crosslinking of the graft films prevents both the initial desorption and subsequent transfer of the PEI, resulting in sustained attractive interaction forces of electrostatic origin between the negatively charged probe and the positively charged copolymer graft films.

© 2004 Elsevier Inc. All rights reserved.

Keywords: Atomic force microscopy; Force measurement; Polymers; Poly(ethylene glycol); Stability; Colloidal-probe AFM

1. Introduction

Poly(ethylene glycol) (PEG) coatings are commonly used in a variety of biotechnology applications to render biomaterial surfaces resistant to protein adsorption [1–3]. The antifouling properties of PEG are the main reason it is used in most applications, but PEG is also used as a tether to flexibly attach active groups to surfaces in biosensing and drug-delivery applications [4,5]. The molecular origin of the protein resistant properties of PEG modified surfaces is still under debate [6–9]. Traditionally, it has been believed that steric forces that arise due to entropic penalties associated with restricted motion of polymer segments were the main forces that prevented contaminant adsorption to PEG surfaces. However, it has recently been acknowledged that hydration forces may play a more significant role in PEG's antifouling efficiency [6]. In any case, it is widely accepted that PEG coatings are inert to protein adsorption and capable

of preserving the activity of the surface [10–12] and, therefore, it is extremely important that the coatings are durable to allow long-term storage and regeneration of the biomaterial surfaces as necessary [13]. Generally, this stability is achieved by covalent end-immobilization of PEG at moderately dense grafting densities.

There are various methods of covalently end-grafting PEG to a surface at a moderate to high grafting density. These methods include: (i) the use of gold–thiol chemistry to covalently attach PEG to gold surfaces [14,15]; (ii) the use of PEG-derivatized block copolymers to graft PEG to hydrophobic surfaces [16,17]; and (iii) the use of silane chemistry [18–20] or the adsorption of amine-rich polyelectrolytes such as polylysine [21,22] and polyethylenimine (PEI) [23,24] to functionalize surfaces with amine groups that will react with amine-reactive PEG derivatives. High molecular weight PEI, a weak cationic polyelectrolyte, has been used to anchor PEG directly to glass and silica surfaces for biosensor applications [11,24]. While the PEG is covalently attached only to the PEI linker molecule, with the PEI linker physisorbed to the surface, such PEG–PEI grafts display the strong, irreversible attachment typically

* Corresponding author. Fax: +1-412-268-7139.

E-mail address: schneider@cmu.edu (J.W. Schneider).

observed for chemisorbed PEGs. PEI and PEG are also used together in gene delivery vectors where the PEI is used to condense DNA while PEG is used to increase the circulation lifetime of these vectors [25,26]. This method of immobilizing PEG to a surface is particularly attractive owing to its cost-effectiveness and the rapid and simple electrostatically driven adsorption of PEI to negatively charged surfaces. For this surface modification procedure, the PEG can either be prereacted with the PEI and the graft copolymer physically adsorbed to the surface, or alternatively the PEG can be grafted onto a preadsorbed PEI layer.

Brink et al. [16,23] have investigated the utility of pre-reacted PEG–PEI adsorbed films on polyethylene. They found that the prereacted copolymer film exhibited superior protein-resistant properties, attributed to an increased mobility of the copolymer-adsorbed layer due to a loop and train conformation. However, the adsorbed layer structure resulted in a few PEG chains being buried in the adsorbed layer and oriented toward the surface, which could sequester active groups linked to the PEG that need to be located at the periphery of the polymer layer. Additionally, the more extended adsorbed layer structure of the PEI may encourage protein adsorption or other biofouling. Therefore, despite the superior antifouling behavior of these adsorbed copolymer films, they have limitations in biosensor technologies that use PEG both for antifouling and for the flexible attachment of biorecognition molecules.

The interfacial properties of PEG films formed by reaction of PEG onto a preadsorbed PEI layer have been studied in some detail. Results from work by Van Alstine et al. [9,24], showed that the adsorption of PEG (MW = 5000 g/mol) at a high grafting density onto a preadsorbed PEI film on quartz shifted the electroosmotic mobility to zero (over a large pH range), and they attributed the protein-resistant nature of PEG coatings, in part, to this observation. Meanwhile, Claesson et al. [27] observed significant steric repulsive interaction forces between PEG–PEI-coated mica surfaces and proposed using the SFA to study interactions between proteins and PEG layers of varying thickness and grafting density. The cited works illustrate the great potential of PEG–PEI graft films as protein-resistant coatings on not just biosensors, but biomaterials in general. However, PEI adsorption studies raise concerns about the stability of the anchoring PEI layer used in these films.

Traditionally, the adsorption of PEI to surfaces has been studied for purification, papermaking, flocculation, and ion-exchange chromatography applications [28–31]. Many of these studies have shown that PEI adsorbs fairly strongly to negatively charged surfaces in a relatively flat conformation and reverses the native surface charge. However, despite the strength of the electrostatic interactions that control PEI adsorption, PEI coatings are somewhat unstable. This has been observed in ion-exchange chromatography where crosslinking modifiers such as glutaraldehyde, alkyl bromides, and nitro alcohols are employed to prevent desorption of PEI from the column packing [31,32]. Although low molecular

weight PEI (MW < 2000) is typically used in the chromatography columns, the unstable nature of adsorbed PEI has also been observed with high molecular weight PEI coatings [9,33,34]. Van Alstine et al. have observed desorption of PEI (MW = 1,800,000) from the quartz capillary walls of their electroosmosis apparatus and suggest glutaraldehyde crosslinking as a means of stabilizing the PEG–PEI graft films [9]. Claesson et al. have also observed desorption and transfer of PEI molecules from PEI films (MW 70,000) in the presence of an uncoated mica surface [33]. Clearly, this reported instability of PEI coatings should be of concern to those interested in using the films as permanent anchoring layers for the immobilization of PEG chains.

Here, we present AFM measurements on the surface properties of PEI, PEG–PEI, and glutaraldehyde-crosslinked PEI/PEG–PEI films adsorbed onto silica. Our choice of silica as a substrate stems from our desire to use a substrate that is commonly used in biotechnology applications. A key question we hope to answer through our force measurements is how the presence of PEG and the crosslinking agent, glutaraldehyde, affects the mechanical stability of PEI molecules. Optical reflectometry is also used to characterize the adsorption properties of PEI onto silica and PEG onto preadsorbed PEI films. The results of our work should serve useful in applications where the stability of the surfaces is imperative for surface regeneration and in the use of the films as antifouling coatings where inertness of the coatings is of great importance.

2. Materials and methods

2.1. Materials

Ultrapure water (18 M Ω cm) obtained using a Milli-Q gradient water filtration system (Millipore, MA) was used for this work. All aqueous solutions were prepared on the day of the experiment. Reagents (Sigma–Aldrich) used to prepare the NaCl solutions and the 50 mM phosphate buffer solutions were of purity >99.9%. A 50% branched-polyethylenimine (PEI) aqueous solution, *Lupasol P*, was obtained from BASF (MW = 750,000 g/mol and manufacturer reported ratio of primary, secondary, and tertiary amine groups of 1:1:1 as determined by NMR spectroscopy). A 5000 g/mol succinimidyl-ester poly(ethylene glycol) derivative (methoxy-PEG-SPA; $M_w/M_n = 1.03$) was purchased from Nektar (Huntsville, AL).

2.2. Treatment of silica substrates

Silicon wafers utilized for optical reflectometry were oxidized for 10–20 min in 1000 °C air yielding a ~30 nm oxide layer. To minimize optical interference, fused silica slides were utilized for the AFM experiments. Both substrates used in the AFM and optical reflectometry experiments underwent a rigorous cleaning treatment that consisted of

exposure to concentrated chromerge (5:1 H₂SO₄:CrH₂O₄) (30 min), dilute 6 M HCl solution (30 min), and 10 mM NaOH (40 min). The silica substrates were then stored in water, dried in a filtered N₂ jet and ozone-cleaned for 30 min prior to use (UVO cleaner, Model 42, JeLight, Irvine, CA).

2.3. Preparation of PEG–PEI coatings

Clean silica substrates were incubated in 500 ppm PEI/50 mM sodium phosphate buffer, pH 7.0 for 2 h at room temperature. The PEI-coated surfaces were then rinsed multiple times with water to remove any weakly adsorbed PEI and dried in a filtered N₂ stream. For PEI–PEG treatment, substrates were incubated with 2.0% (w/v) methoxy-PEG-SPA/50 mM sodium phosphate buffer, pH 7.0 for 2 h at 37 °C. Glutaraldehyde crosslinking of PEI and PEG coatings was accomplished by incubating the surfaces in 1% glutaraldehyde (Sigma–Aldrich), 0.5 mg sodium cyanoborohydride (Sigma–Aldrich) per 10 ml of solution, 50 mM sodium phosphate buffer, pH 7.0 for 12 h at room temperature [9].

2.4. Optical reflectometry

Optical reflectometry was utilized to characterize the surface coverage of both PEI on silica and PEG on PEI-coated (500 ppm) silica in 50 mM sodium phosphate buffer over a 2-h adsorption period. The cell was rinsed with water for about 30 min after 2 h to remove any nonadsorbed polymer.

This optical reflectometry method has been described in detail elsewhere [35–38]. The technique is based on illuminating an interface with p-polarized light at a fixed angle of incidence equal to the Brewster angle and recording the reflectivity of the interface. The surface excess concentration is approximated from the difference between the reflectivity ($R_p(\theta_B, \Gamma)$) after adsorption and the initial reflectivity of the bare interface ($R_p(\theta_B, 0)$):

$$\Gamma = \alpha [R_p(\theta_B, \Gamma)^{1/2} - R_p(\theta_B, 0)^{1/2}]. \quad (1)$$

In the approximation above, the proportionality constant α is calculated from a striated interface optical model, using the oxide layer thickness measured prior to the adsorption. Eq. (1) is valid up to surface excess concentrations of about 3 mg/m², which is a suitable upper limit for the adsorption of the polymers we use in our studies. The reflectometry instrument consists of a rectangular slit-flow cell with the silicon wafer as the lower face and one face of a fused-silica prism forming the upper wall. A HeNe laser beam is used and for the methoxy-PEG-SPA adsorption studies, the flow cell housing is maintained at constant temperature by circulating thermostated water (at 37 °C) through the housing.

2.5. Atomic force microscopy (AFM)

Force measurements were conducted in a Nanoscope III multimode AFM using Si₃N₄ cantilevers of nominal spring

constants between 0.01 and 0.03 N/m (Veeco Metrology, Santa Barbara, CA). For all measurements, the integral tip usually available as a probe was modified by attachment of a silica microsphere with mean diameter of 5 μ m (Bangs Laboratories, Fisher, IN) to the base of the tip using a low viscosity UV-curing glue (Norland Products, Cranberry, NJ) [39]. Before use, the cantilevers underwent UV-ozone cleaning for 35 min. All force measurements were conducted in solutions of either pure water, 0.5 mM NaCl, or 50 mM NaCl. Between 100 and 200 force curves were collected at various positions on the surface and experiments were repeated to confirm the reproducibility of the data obtained.

Details about AFM force measurements are available elsewhere [39–42]. We utilize the standard method of calibrating the probe-sample separation by assuming the onset of linear cantilever deflection or “constant compliance region” corresponds to zero separation with respect to the origin of polymer attachment. The constant compliance region may be reached before the probe makes intimate contact with the surface if the compressed stiffness of polymer underneath the probe exceeds the compliance of the cantilever. In this case, the constant-compliance region will occur at a distance above the underlying substrate corresponding to the thickness of incompressible polymer (D_0), and the calculated separation distance between the probe and the origin of attachment will be in error by a factor of D_0 . In recognition of this, we emphasize that these separation distances, D , are apparent separations and not absolute separations with respect to the origin of polymer attachment.

Owing to the large number of surfaces studied in this paper, we will adopt the following reference format to define the interacting surfaces: (surface 1:surface 2). Here, surface 1 is the planar surface and surface 2 is the spherical probe. Two types of force measurements were conducted on all the films: (i) force measurements between identical films that we term “symmetric” and (ii) force measurements between a polymer-coated planar surface and an uncoated silica sphere that we term “asymmetric.” The reported units of all the force measurements are in terms of a scaled force, where the force is scaled by the probe radius (F/R).

Height images of the swollen polymer-coated surfaces were also obtained using tapping-mode AFM. For this image collection, Si₃N₄ cantilevers with a nominal spring constant of 0.5 N/m and tip radii of 25–40 nm were utilized. Polymer layer heights were approximated from imaged height differences between the layer and surface defects that were natural or that were promoted by mechanical scratching.

3. Results and discussion

3.1. Adsorption studies

The final adsorbed amounts after a 2-h incubation period of three different dilute PEI solutions in the 50 mM phosphate buffer, pH 7.0 is shown in Fig. 1a. The amount

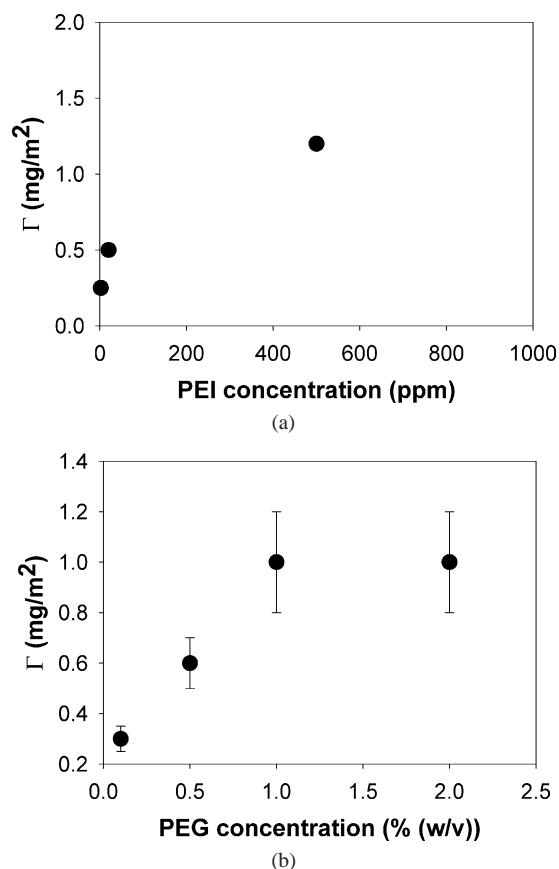


Fig. 1. (a) Adsorption behavior of PEI in 50 mM phosphate buffer, pH 7.0 onto silica. (b) Adsorption behavior of PEG in 50 mM phosphate buffer, pH 7.0 onto a preadsorbed PEI (500 ppm) film.

adsorbed increases with the concentration of the PEI bulk solution. At pH 7, we expect about 45% protonation of the amine groups on the PEI [43]. Therefore, we expect intrasegment and intermolecule electrostatic repulsion to occur. However, at the high ionic strength of the solution used, this repulsion should be sufficiently screened. The adsorption isotherm suggests that the surface does not become saturated until some critical concentration that occurs close to 500 ppm. Though scaling theories exist to describe the adsorption of linear strongly charged polyelectrolytes, there are currently no such theories for the adsorption of weakly charged, branched polyelectrolytes. Therefore, we cannot accurately estimate the adsorbed layer thickness of the PEI based on the adsorbed amount data. Instead, we will rely on AFM images to obtain an estimate of the layer thickness of the adsorbed PEI layer obtained from the 500 ppm bulk PEI solution.

The covalent grafting of PEG to the PEI anchor layer is achieved through ester–amine reaction chemistry—the amine groups are present on the PEI and the PEG is derivatized with a succinimidyl ester functional group. A complicating factor is that this reaction depletes the number of amine groups on the PEI that can interact with the silica surface. However, because we use PEI of very large molecular weight, we do not believe that this depletion of potential sur-

face binding sites is significant enough to greatly affect the interaction of the PEI with the silica or its conformation on the surface.

The final adsorbed amounts Γ of methoxy-PEG-SPA onto the preadsorbed PEI film (prepared from 500 ppm PEI solution) achieved after a 2-h incubation period are shown in Fig. 1b and vary from 0.3 mg/m² at the lowest bulk concentration to a saturation adsorbed amount of 1 mg/m² at the highest bulk concentrations (above 1.0% PEG (w/v)). These adsorbed amounts correspond to an end-to-end distance s ($s = \Gamma^{-2}$) between grafting points that varies from 5.3 to 2.9 nm. Comparing these values of s to the estimated Flory radius R_f (6.1 nm) [44], representative of the size of the polymer coil in good solvent, we find we can vary the adsorbed layer conformation through changes in the bulk adsorbing PEG concentration.

The two main conformations for grafted layers are the “mushroom-like” conformation ($s \geq R_f$), in which the chains maintain a coil-like conformation analogous to their solution conformation, and a “brush-like” conformation ($s < R_f$) in which the chains extend out into solution. For our PEG layers, the highest grafting density (smallest distance between grafting points) obtainable is estimated to be $s = 1$ nm, under the assumption that the PEG derivative reacts with all available primary amine groups on the PEI (located at the end of the branch points). The manufacturer estimates approximately two ethylenimine units between branch points. As observed in the experiments, the smallest end-to-end distance between grafting points attainable is 3 nm. The deviation between this value and the ideal end-to-end distance calculated can be attributed to steric influences due to the highly branched nature of the PEI. Despite this deviation, we expect that the grafting density Γ obtained at these concentrations yields moderately extended PEG chains on the PEI film. From Alexander’s scaling theory for polymer brushes in good solvent, at saturation the expected PEG brush thickness L_B is about 10 nm [45]:

$$L_B = \Gamma^{1/3} R_f^{5/3}. \quad (2)$$

While Eq. (2) assumes anchorage in a plane, these PEG chains may be anchored at different depths within the diffuse PEI layer. However, due to the expected flat conformation of the PEI layer and steric hindrances, we believe that approximating the PEG anchorage to be planar is not unreasonable. Since $L_B > R_f$, this indicates a moderate extension of PEG chains from the surface (Fig. 2). Layers of this grafting density are used in the force measurements described later as they suitably mimic the types of layers used in biosensor applications.

3.2. Tapping-mode AFM images of surfaces

Tapping-mode AFM images of the 500 ppm PEI film show a flat and smooth layer of fairly homogeneous coverage (Fig. 3a). This smooth and flat coverage was also observed for the 2 and 20 ppm PEI films. There are some small

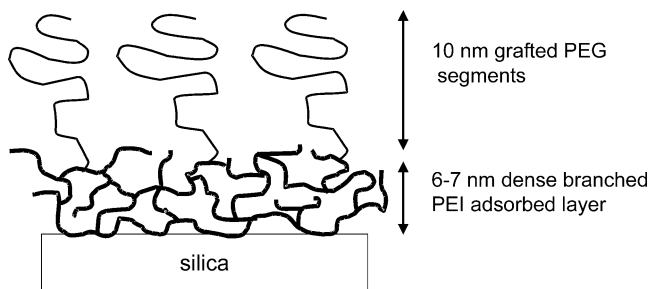


Fig. 2. Schematic of proposed conformation of PEI-PEG copolymer graft on the silica surface.

empty patches where no PEI adsorbed and from the step difference between these areas and the rest of the layer, we estimate a film thickness of about 6–7 nm. This agrees well with the film thickness (7–8 nm) obtained by mechanically scratching the surface with a tip in contact-mode AFM at high loads. Therefore we use this thickness as an estimate of the compressed PEI thickness. We estimate the solution size of the PEI molecules to be around 30 nm based on light scattering data of PEI polymers [46,47]. The observation that the layer thickness is much smaller than the characteristic size of the molecule in solution reinforces the hypothesis that PEI is adsorbed in an overall flat conformation. The PEG-PEI films in contrast, are less smooth and consist of globular domains (Fig. 3b). These domains are typically observed for PEG coatings [18].

3.3. Force measurements on PEI films

Symmetric force measurements at low ionic strength conditions were used to quantify the magnitude of charge on the surfaces. These force measurements were first conducted between a silica flat and silica probe as a reference and the scaled force as a function of apparent separation D is shown in Fig. 4. The long-range interaction is attributed to electrostatic double layer forces. Theoretical fits based on the algorithm of Chan et al. [48] (constant-charge condition) yield a Debye length κ^{-1} of 54 nm or an ionic strength of the order of 10^{-5} M (assuming a 1:1 electrolyte) which is reasonable for the purity of the water used. A fitted surface potential ϕ_s of -39 mV is obtained (see Table 1). We assign a negative sign for ϕ_s for the two interacting silica surfaces as the surrounding pH (~ 5.3) is above silica's isoelectric point (pH ~ 3) [29] and therefore we expect dissociation of the silanol groups on the silica. We assume that the silica microsphere and fused silica surface are chemically identical and neglect a complete DLVO fit to the force curves due to the uncertainty in the value of the Hamaker constant for measurements on the polymer-covered surfaces.

3.3.1. (PEI:PEI)

Symmetric force measurements displayed a larger long-range interaction than that observed with silica even at very low concentrations of PEI used for adsorption (Fig. 4). Fitted ϕ_s at the interface between the adsorbed polyelectrolyte and

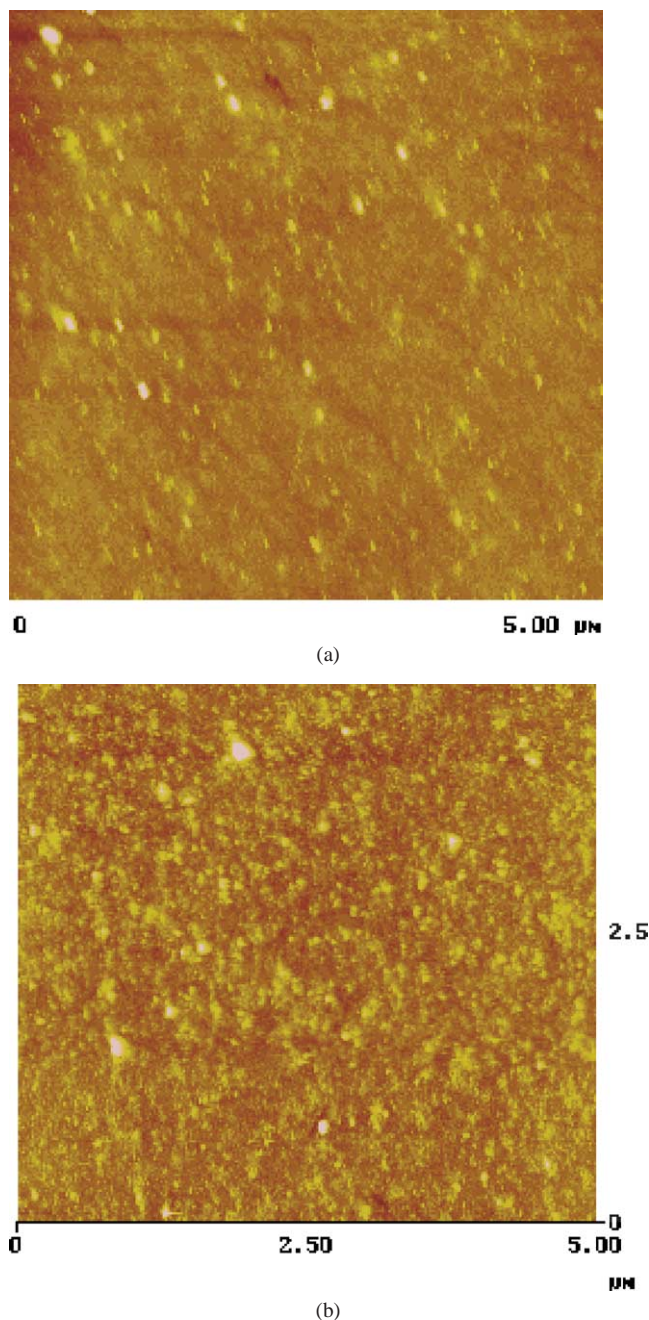


Fig. 3. (a) TM-AFM height image of a PEI film (adsorbed from 500 ppm). (b) TM-AFM height image of a PEG film (from 500 ppm PEI, 2.0% (w/v) PEG). Both images were taken over a over a $25 \mu\text{m}^2$ area with a vertical scale of 20 nm.

the solution for the PEI-coated surfaces adsorbed from 2, 20, and 500 ppm PEI range narrowly from 57 to 61 mV respectively with fitted values for κ^{-1} that yield ionic strengths of the order of 10^{-5} M (Table 1). This indicates that the native charge of the silica is reversed at very dilute concentrations of PEI and supports previous work that showed that very low concentrations of PEI result in a shift in the isoelectric point (IEP) of the silica to very basic pH due to surface complexation reactions [30]. The significant overcompensa-

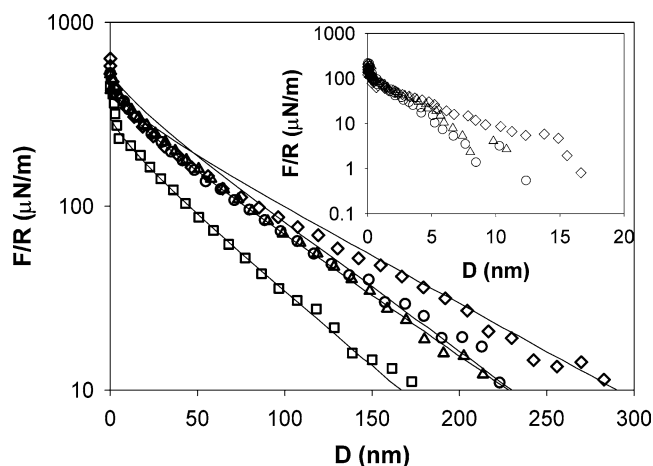


Fig. 4. Force (scaled by probe radius) versus separation for interacting silica surfaces and interacting PEI layers (PEI:PEI), adsorbed from varying bulk concentrations: bare silica (\square), 2 ppm PEI (Δ), 20 ppm PEI (\circ), 500 ppm PEI (\diamond) in water. The force curves were fit (solid lines) to calculated electrostatic force curves based on the Poisson–Boltzmann equation using constant-charge boundary conditions [48]. The values of the fit parameters are shown in Table 1. Inset: Scaled force versus separation for interacting PEI layers in 50 mM NaCl.

tion of the substrate charge has been also attributed to the branched state of the PEI molecules that results in a dense amount of charge in the small surface area that the molecule adsorbs to [49]. Although the plane of charge is not well defined for these polyelectrolyte adsorbed layers, Claesson et al. have shown that hardly any polyelectrolyte is present in the diffuse double layer due to a “depletion zone” that develops outside the surface because of the like charge of the two polyelectrolyte-coated surfaces [33]. Therefore, we will assume that the PEI chains minimally affect the electrostatic decay length. We further define the plane of charge to coincide with the highly compressed polymer layer thickness and not the silica substrate. Therefore, the narrow change in

surface potential at the various concentrations suggests that the segment density profiles of each compressed adsorbed layer are not concentration dependent and that all layers are therefore most likely in a relatively flat conformation. However, the deviation in the decay length of the 500 ppm film suggests a greater density of tails in this layer.

Not surprisingly, only the force measurements on the 2 ppm PEI layer exhibit hysteresis between the approach and retract interaction profiles. For this layer, the retract curves exhibit a scaled adhesive force of magnitude $\sim 40 \mu\text{N/m}$ and consistent jump-out distances of about 15 nm relative to the “constant-compliance region.” This adhesion upon retraction persists over most of the force curve collection and is most likely due to bridging of polymer segments during compression to empty patches on the opposing surface [50]. This adhesion, as expected, is absent at higher PEI bulk concentrations in which both surfaces are more densely covered.

Measurements were also conducted in 50 mM NaCl to verify the electrostatic origins of the long-range interactions observed in water and to elucidate the differences in layer structure of the various PEI films. Scaled force versus separation curves for the various PEI adsorbed layers in electrolyte are shown in the inset of Fig. 4. The interactions remain repulsive but are now significantly shorter-ranged with decay lengths at $D < 2 \text{ nm}$ of $\kappa^{-1} = 2.45 \text{ nm}$ (2 ppm PEI), 1.33 nm (20 ppm PEI), and 1.7 nm (500 ppm PEI) and $\kappa^{-1} = 2.49 \text{ nm}$ (2 ppm PEI), 2.46 nm (20 ppm PEI), and 4.45 nm (500 ppm PEI) at $D > 2 \text{ nm}$. The Debye length of the surrounding medium κ_s^{-1} is 1.36 nm, therefore repulsions of larger decay lengths can be attributed to the added contribution of polymer steric forces. From these results, it is clear that all the adsorbed layers exhibit a steric barrier against compression. This steric barrier remains constant at all separations for 2 ppm PEI indicating a loop-train conformation with a high-density of loops and few tails. From the

Table 1
Fitted surface potentials of the various interacting surfaces

Surface 1	Surface 2	Electrolyte (NaCl)	ϕ_1 (mV)	ϕ_2 (mV)	κ^{-1} (nm)
Symmetric measurements					
Si	Si	None	−39	−39	54
PEI (2 ppm)	PEI (2 ppm)	None	+57	+57	61
PEI (20 ppm)	PEI (20 ppm)	None	+56	+56	65
PEI (500 ppm)	PEI (500 ppm)	None	+61	+61	81
PEG–PEI ^a	PEG–PEI ^a	None	+49	+49	63
Crosslinked PEI ^a	Crosslinked PEI ^a	None	+41	+41	45
Asymmetric measurements					
Si	PEI (500 ppm)	None	–	–	32
Si	PEG–PEI ^a	None	+15	+55	36
Si	Crosslinked PEI ^a	None	−40	+62	34
Si	Crosslinked PEI ^a	0.5 mM	−40	+7	13
Si	Crosslinked PEI ^a	Water reflush after 50 mM	−40	+62	19
Si	Crosslinked PEG ^a	None	−40	+38	34
Si	Crosslinked PEG ^a	0.5 mM	−40	+5	12
Si	Crosslinked PEG ^a	Water reflush after 50 mM	−40	+20	19

^a Surfaces were prepared with a preadsorbed PEI (500 ppm) film.

difference in the fitted decay lengths below and above 2 nm, it appears that increasing the adsorbing PEI concentration past 2 ppm results in conformations with a lower density of loops resulting in a negligible steric barrier ($\kappa^{-1} \approx \kappa_s^{-1}$) at small separations (20 ppm PEI) but with an increasing density of tails which further increases with increased PEI bulk concentration (500 ppm PEI). These conformational characteristics are well described by the theoretical model based on mean-field lattice theory developed by Linse [51]. This model predicts that a 10-fold increase in bulk polymer volume fraction results in adsorbed conformations where the tail lengths almost double and the loop length remains constant but with a 20% decrease in the number of loops present. Additionally, the fraction and length of trains remain unchanged.

Similar to the force measurements in salt-free solution, there was little hysteresis in approach and retract curves on the 20 ppm and 500 ppm PEI surfaces. The magnitude of the scaled adhesive force ($\sim 40 \mu\text{N/m}$) and jump-out distances (12–16 nm) observed upon retraction for the 2 ppm PEI surface were comparable to those seen in water. This suggests a similarly structured and already compact layer in both conditions. Again, we attribute the origin of this adhesion to bridging of the segments across the surfaces that is promoted during compression.

3.3.2. (PEI:silica)

Asymmetric force measurements were also collected for the 500 ppm PEI film. It is this bulk PEI concentration that is used to form the PEG–PEI graft films and the crosslinked PEI film discussed in the last section. Single force curves were collected for the first contact between the probe and sample and a few subsequent contacts, then the approach/retraction cycle of the probe was made continuous (at a rate of 1 Hz) for subsequent force curve collection. The scaled force versus separation for measurements between a silica microsphere and the PEI film with increasing contact is shown in Fig. 5.

A long-range repulsion is observed followed by a short-ranged attraction at small separations that decreases with subsequent contact. The existence of a long-range repulsion is surprising and the only reasonable explanation for this observation (assuming electrostatic origins) is that some PEI desorbed from the coated surface and fouled the probe causing charge reversal of the native silica charge. Sidorova et al. [30] have shown that a very low concentration of PEI adsorbed to fused quartz can dramatically shift its isoelectric point to 8, resulting in the reversal of the sign of the surface charge from negative to positive. Therefore, the interaction between the fouled probe and PEI surface is akin to the interaction between two surfaces of like charge. Further, when the scaled force versus separation curves approach constant repulsion (indicating no further transfer), a theoretical fit using constant-charge boundary conditions and equivalent potentials on both surfaces, yields a surface potential of +27 mV, corroborating some loss of PEI from the sample

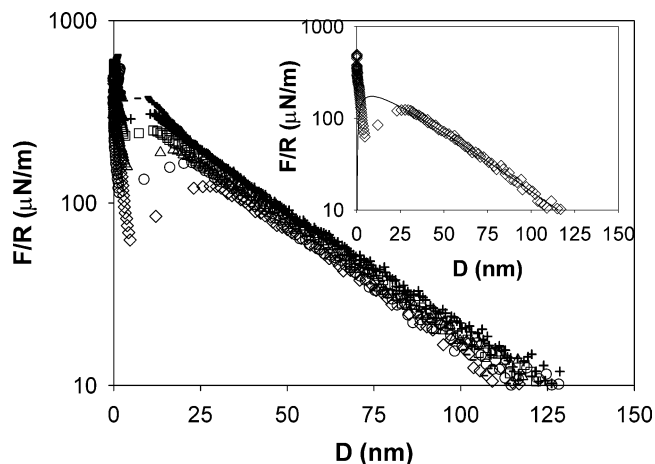


Fig. 5. (PEI:silica) Scaled force versus separation for an uncoated microsphere (1) interacting with a PEI-coated slide adsorbed from 500 ppm PEI (2) in water: 1st contact (\diamond), 2nd contact (\circ), 4th contact (Δ), 18th contact (\square), 116th contact ($+$), and 212th contact ($-$). Inset: Theoretical fit to the 1st contact curve (solid line) using constant potential boundary conditions ($\kappa^{-1} = 32 \text{ nm}$; $\phi_1 = 27 \text{ mV}$ and $\phi_2 = 60 \text{ mV}$).

surface. Desorption can be traced to two possible sources: (i) the lowering of pH between the adsorbing conditions and the measurement conditions that would result in a decrease in the electrostatic attraction between the silica and PEI, causing PEI expansion and desorption [9]; and (ii) the desorption of PEI molecules due to the drying step. Extensive experiments with PEI films adsorbed and measured at the same pH (5.3) and with nondried PEI films show initial desorption and subsequent contact-initiated transfer occurring in all cases (not shown). Therefore, it seems that this desorption of PEI molecules is spontaneous with both desorbed and adsorbed PEI molecules favoring adsorption onto the negatively charged microsphere. The short-range attraction in the force curves could not be fit to double-layer theory using constant-potential boundary conditions (see inset of Fig. 5). Constant-charge conditions were not used because they lead to purely repulsive double-layer forces [52]. We attribute this short-range attraction to be due to bridging promoted by a patch charge attraction between the surfaces [33,50,53].

The strong attraction between the segments and the bare surface is seen in the retract curves, in which very strong scaled adhesive forces are observed (Fig. 6). With subsequent contact (at scaled forces between 300 and 500 $\mu\text{N/m}$ or contact energies reaching $10^3 k_B T$ and a contact area of 20 nm), more PEI molecules transfer to the probe and fill up the empty patches resulting in the disappearance of both the short-ranged attraction on approach and a reduction in the magnitude of the scaled adhesive force upon retraction (Fig. 6). There is also a small but noticeable increase in the magnitude of repulsion observed that likely has both electrostatic and steric origins. Similar interaction force profiles were observed in surface force apparatus experiments for a bare mica surface interacting with a PEI-coated mica surface [33].

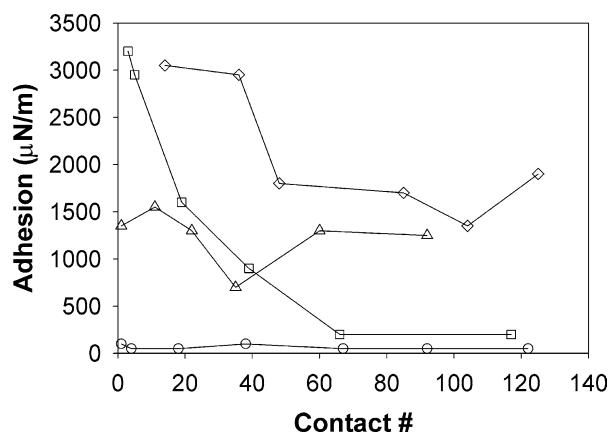


Fig. 6. (PEI, PEG-PEI, xPEI, xPEG-PEI:silica) Scaled adhesive force upon retraction with increasing number of contacts between the bare probe and 500 ppm PEI (□), PEG-PEI graft film (○), crosslinked 500 ppm PEI (◇), and crosslinked PEG-PEI graft film (△) in water.

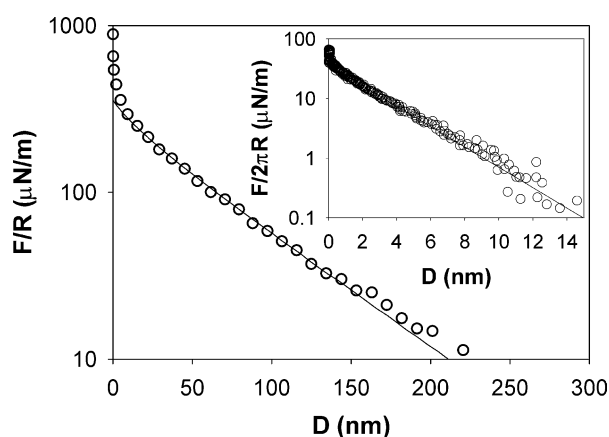


Fig. 7. (PEG-PEI:PEG-PEI) Scaled force versus separation for two interacting PEG-PEI graft films prepared from 500 ppm PEI and 2.0% (w/v) PEG (○) in water. Inset: $F/2\pi R$ (Derjaguin's approximation [54]), equivalent to the energy of interaction between the two planar PEG-covered surfaces in 50 mM NaCl as a function of separation. The solid line is a theoretical fit based on (4).

3.4. Force measurements on PEG-PEI graft films

3.4.1. (PEG-PEI:PEG-PEI)

Symmetric force measurements were also conducted between PEG-PEI grafted films in water and 50 mM NaCl solution to characterize the surface charge and the structural properties of these surfaces. The interactions in water displayed a long-range behavior characteristic of electrostatic double-layer forces (Fig. 7), and the magnitude of the surface potential obtained from theoretical fits was only slightly lower than that obtained on the native PEI film (Table 1). The decrease in the fitted surface potential may be attributed to an increase in the thickness of incompressible polymer (due to the additional PEG layer) that shifts the reference point for zero separation further away from the origin of the PEI surface charge.

In 50 mM NaCl, the interaction forces were dominated again by steric repulsion as shown in the inset of Fig. 7. The

curve was fit to an exponential approximation of the model developed by Alexander-de Gennes that quantifies the surface pressure felt between two interacting neutral polymer brushes [54]:

$$\frac{F(D)}{R} = \frac{100kTL_B}{\pi s^3} e^{-\pi(D-D_0)/L_B}. \quad (3)$$

The distance between graft sites (s) was set to 3 nm based on the optical reflectometry results. Therefore, only the thickness of incompressible polymer (D_0) and the brush height (L_B) were the adjustable parameters. From the fit, $L_B = 8$ nm and $D_0 = 18$ nm. If we ascribe 6–7 nm of $D_0/2$ (obtained from AFM imaging) to an incompressible PEI layer, we obtain an uncompressed PEG brush height of about 10–11 nm, which agrees reasonably well with that predicted from scaling theory [45] based on the adsorbed amount obtained from optical reflectometry.

For these symmetric measurements between PEG-coated surfaces, multiple adhesive events were sometimes observed in retract curves in both the water and salt solutions indicating bridging of polymer segments between the surfaces. Jump-out distances extending beyond the contour length of the PEG chains (42 nm) were occasionally observed indicating the additional stretching of PEI anchoring segments. The frequency of adhesion hysteresis in salt was about 44% and that in water was about 4% of total force curves taken. Since we do not observe adhesion hysteresis in the interaction between PEI-coated surfaces in 50 mM NaCl, this suggests that the driving force for bridging is due to favorable interactions between PEG and itself and PEG and PEI segments that only occur once the long-range electrostatic repulsive barrier is screened. 50 mM NaCl is a good solvent for PEG molecules [55], but it is possible that the solvent quality for the copolymer graft is worsened in 50 mM NaCl thereby driving the bridging phenomena.

3.4.2. (PEG-PEI:silica)

When asymmetric force measurements are conducted between an uncoated silica sphere and a PEG-PEI-coated surface in water, a long-range repulsion and a short-range attraction are also observed (Fig. 8). With subsequent contact, the attraction persists contrary to that observed in the asymmetric force measurements on the PEI films. The observation of long-ranged repulsion is again indicative of charge reversal of the silica probe due to desorption of PEI segments from the sample with re-adsorption onto the probe. The scaled force versus separation profile obtained on these PEG-PEI surfaces can be fit using constant-potential boundary conditions with dissimilar but like-charged surface potentials (see inset of Fig. 8). This attractive double layer force for like but unequally charged surfaces is specific to the assumption of constant potential boundary conditions [52, 56,57]. For these boundary conditions, the surface potential is maintained constant through the adsorption or desorption of counterions from the surfaces. The attraction at small distances occurs when there is a reversal in charge of the surface

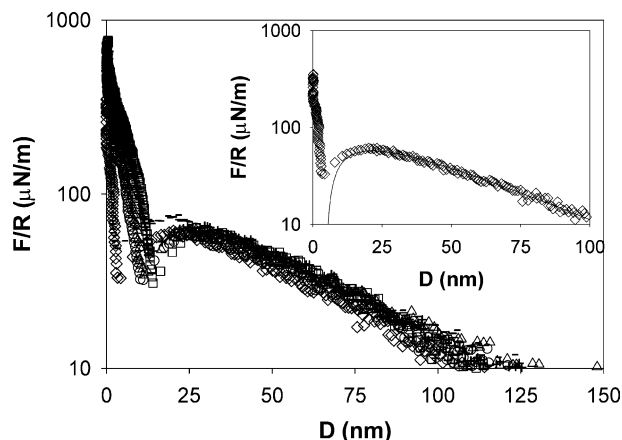


Fig. 8. (PEG-PEI:silica) Scaled force versus separation for an uncoated microsphere (1) interacting with a PEG-coated slide grafted from 500 ppm PEI and 2.0% (w/v) PEG (2) in water: 1st contact (\diamond), 4th contact (\circ), 27th contact (Δ), 67th contact (\square), 105th contact ($+$), and 168th contact ($-$). Inset: Theoretical fit (solid line) using constant potential boundary conditions ($\kappa^{-1} = 36$ nm; $\phi_1 = 15$ mV and $\phi_2 = 55$ mV).

of smaller potential due to induced charge from the surface of larger potential [57]. Therefore, for the interactions between the bare probe and the PEG-PEI-coated surface, it appears that some initial desorption of PEI or PEI-PEG still occurs (fouling the probe), but the presence of the PEG on the surface reduces further transfer of PEI molecules resulting in an interaction between two constant potential surfaces. Correspondingly, the presence of PEG chains is found to significantly decrease the adhesive interaction of the PEI with the uncoated probe as observed through a decrease in the magnitude of the scaled adhesive force F_{adh}/R on retraction on PEG-PEI graft films. F_{adh}/R is approximately 2400 $\mu\text{N}/\text{m}$ for the native PEI film and decreases to about 80 $\mu\text{N}/\text{m}$ for the PEG-PEI graft film (Fig. 6).

3.5. Force measurements on crosslinked surfaces (xPEI and xPEG-PEI)

In an effort to prevent desorption of PEI that causes initial fouling of the probe, the PEI- and PEG-coated surfaces were crosslinked using glutaraldehyde [9].

3.5.1. (xPEI:silica)

Asymmetric scaled force versus separation curves for the interaction between an uncoated silica sphere and a crosslinked PEI-coated surface are shown in Fig. 9. In water, the interaction is a long-range attraction that is sustained with subsequent contact. When the solution is changed to 0.5 mM NaCl, the attraction becomes more short-ranged with the decay of the attraction equivalent (within 10%) to the Debye length expected for this ionic strength ($\kappa_s^{-1} = 13.6$ nm). Upon further increase of the electrolyte concentration to 50 mM NaCl ($\kappa_s^{-1} = 1.36$ nm), the attraction disappears and only a short-range steric repulsion remains that becomes significant at separations smaller than 8 nm (see inset of Fig. 9). Reflushing the cell with water results in

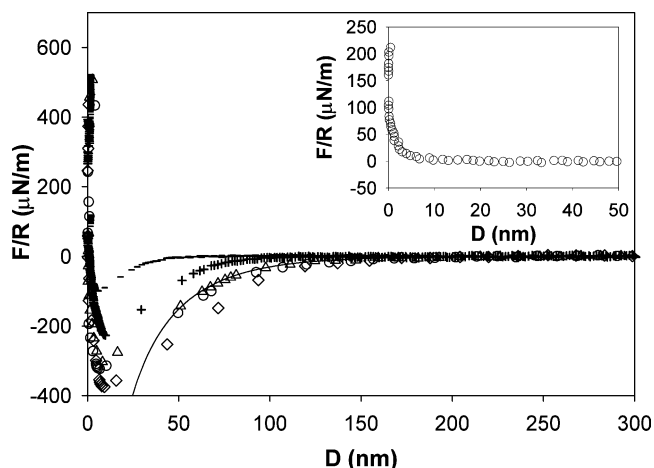


Fig. 9. (xPEI:silica) Scaled force versus separation for an uncoated microsphere (1) interacting with a glutaraldehyde-crosslinked PEI-coated slide adsorbed from 500 ppm PEI (2) in water: 36th contact (\diamond), 85th contact (\circ), 125th contact (Δ) in water. Solid line is the attempted theoretical fit using constant potential boundary conditions. Measurements in 0.5 mM NaCl ($-$), 50 mM NaCl (inset), and reflush with water ($+$) are also shown.

the immediate renewal of the long-range attraction with a decay length of 19 nm proving that the origin of the attraction is electrostatic and that crosslinking the PEI with glutaraldehyde does indeed prevent any desorption or transfer of the PEI. To further confirm the electrostatic origins of the attraction, symmetric force measurements were conducted between a crosslinked PEI-coated sphere and a crosslinked PEI-coated surface (xPEI:xPEI). The result was a long-range electrostatic repulsion between the two surfaces as expected (not shown).

The long-range attractions observed between the bare sphere and crosslinked PEI surface can be theoretically fit with the assumption of a fixed surface potential for the bare microsphere ($\phi_1 = -40$ mV), that is averaged from several surface potential fits to interaction forces obtained between clean silica surfaces in previous experiments. The resulting fitted surface potential (ϕ_2) is shown in Table 1. We must emphasize that this fitted potential is for comparative purposes only. We recognize that changes in the ionic strength will result in a decrease in the surface potentials of both surfaces.

3.5.2. (xPEI-PEG:silica)

A similar long-range attraction is seen for asymmetric force measurements between the silica sphere and the crosslinked PEG-PEI-coated surface (Fig. 10). The interaction also follows the same behavior when 0.5 mM NaCl is added with an expected decrease in the range of the attraction. However, with addition of 50 mM NaCl, the interaction remains attractive with an onset that is comparable in length to the brush height of the PEG chains (see inset of Fig. 10). This attraction likely stems from the favorable interaction energy between the PEG segments and the silica probe [58]. Upon reflushing the cell with water, the long-range attraction reappears. From the fitted surface potentials

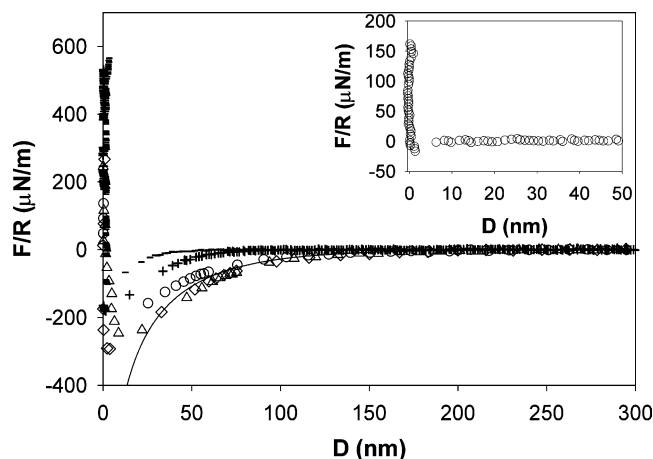


Fig. 10. (xPEG–PEI:silica) Scaled force versus separation for an uncoated microsphere (1) interacting with a glutaraldehyde-crosslinked PEG-coated slide grafted from 500 ppm PEI and 2.0% (w/v) PEG (2) in water: 11th contact (\diamond), 35th contact (\circ), 92nd contact (\triangle) in water. Solid line is the attempted theoretical fit using constant potential boundary conditions. Measurements in 0.5 mM NaCl ($-$), 50 mM NaCl (inset), and reflux with water ($+$) are also shown.

(Table 1), it is interesting to note that the surface potential of the crosslinked PEG–PEI-coated surface is not completely regenerated after the water reflux, though the experimental Debye length of the interaction is identical to that of the crosslinked PEI-coated surface. This suggests that there are some counterions introduced with the 50 mM NaCl that are strongly bound to the polymer matrix.

3.5.3. (xPEI:silica, xPEG–PEI:silica)

When probing both the PEI and PEI–PEG crosslinked surfaces with the uncoated silica sphere, the scaled adhesive force on retraction is fairly large and we attribute this to the strong electrostatic attraction between the oppositely charged surfaces (Fig. 6). With an increase in ionic strength, this force (scaled) decreases significantly from an average value of 1600 and 1000 $\mu\text{N/m}$ in water, to 400 and 292 $\mu\text{N/m}$ in 0.1 mM NaCl, and 0 and 40 $\mu\text{N/m}$ in 50 mM NaCl for the crosslinked PEI and PEG surfaces, respectively. The observed decrease with ionic strength is due to the screening of the electrostatic attraction between the two surfaces as the ionic strength is increased. Particularly, in 50 mM NaCl where the interaction range for electrostatics has been sufficiently screened to <1.5 nm, the scaled force appropriately coincides with that observed on the respective noncrosslinked surfaces.

4. Summary

From our AFM force measurements, we have been able to elucidate some important interfacial properties of PEI, PEG–PEI, and glutaraldehyde-crosslinked PEI and PEG–PEI films. From asymmetric measurements, we have observed both spontaneous and load-induced desorption of

adsorbed, uncrosslinked PEI molecules when probed with a bare microsphere. The typical scaled contact forces for which transfer was observed were on the order of 400 $\mu\text{N/m}$. The presence of PEG chains increases the stability of the coating by preventing load-induced desorption, and reduces the adhesive nature of the native PEI film. However, the complete elimination of initial desorption and progressive transfer can only be achieved using crosslinking modifiers such as glutaraldehyde. This implies that the stability of PEI-derived coatings is dependent on the number of free amines present in the molecule and the flexibility of the adsorbed molecule.

From symmetric measurements, we have also characterized the surface charge of PEG–PEI films and observed that these films have an excess positive charge arising from the cationic PEI sublayer. This surface charge should be considered in the use of PEG–PEI films at low ionic strengths where the charge may affect the specific binding of proteins and the nonspecific adsorption of contaminants in applications such as biosensors. Under moderate ionic strength conditions, the electrostatic interactions are screened and the films exhibit a fairly large steric force that may assist in the inhibition of protein adsorption in biofouling applications. We have additionally observed that the crosslinked PEG–PEI films exhibit a significant steric force against compression at these conditions, but often favorable attraction between the negatively charged probe and PEG segments dominate the interaction.

In conclusion, this study demonstrates a need to scrutinize PEG–PEI surface preparation methods before implementing them in various applications. Such scrutiny may include AFM force measurements of this type.

Acknowledgments

The authors acknowledge the ACS Petroleum Research Fund (Grant 37734-G7) and the National Science Foundation (Grant CTS-0210205) for financial support of this work. We also thank Simon Biggs for helpful discussions and Alan Braem for the electrostatic fitting algorithm.

References

- [1] G.N.C. Chiu, M.B. Bally, L.D. Mayer, *Biochim. Biophys. Acta* 1510 (2001) 56.
- [2] N.A. Alcantar, E.S. Aydil, J.N. Israelachvili, *J. Biomed. Mater. Res.* 51 (2000) 343.
- [3] E. Tziampazis, J. Kohn, P.V. Moghe, *Biomaterials* 21 (2000) 511.
- [4] J.M. Harris (Ed.), *Poly(Ethylene Glycol) Chemistry—Biotechnical and Biomedical Applications*, Plenum, New York, 1992.
- [5] B.K. Mann, R.H. Schmedlen, J.L. West, *Biomaterials* 22 (2001) 439.
- [6] M. Morra, *J. Biomater. Sci. Polym. E* 11 (2000) 547.
- [7] D. Leckband, S. Sheth, A. Halperin, *J. Biomater. Sci. Polym. E* 10 (1999) 1125.
- [8] M. Morra, C. Cassinelli, *Colloids Surf. B* 18 (2000) 249.
- [9] N.L. Burns, J.M. Van Alstine, J.M. Harris, *Langmuir* 11 (1995) 2768.

- [10] R.L. Edelstein, C.R. Tamanaha, P.E. Sheehan, M.M. Miller, D.R. Baselt, L.J. Whitman, R.J. Colton, *Biosens. Bioelectron.* 14 (2000) 805.
- [11] S.W. Metzger, M. Natesan, C. Yanavich, J. Schneider, G.U. Lee, *J. Vac. Sci. Technol. A* 17 (1999) 2623.
- [12] N. Xia, Y. Hu, D.W. Grainger, D.G. Castner, *Langmuir* 18 (2002) 3255.
- [13] O. Birkert, H.-M. Haake, A. Shütz, J. Mack, A. Brecht, G. Jung, G. Gauglitz, *Anal. Biochem.* 282 (2000) 200.
- [14] R.M. Nyquist, A.S. Eberhardt, L.A. Silks III, Z. Li, X. Yang, B.I. Swanson, *Langmuir* 16 (2000) 1793.
- [15] H.B. Lu, C.T. Campbell, D.G. Castner, *Langmuir* 16 (2000) 1711.
- [16] K. Holmberg, F. Tiberg, M. Malmsten, C. Brink, *Colloids Surf. A* 123–124 (1997) 297.
- [17] D. Muller, M. Malmsten, S. Tanodekaew, C. Booth, *J. Colloid Interface Sci.* 228 (2000) 326.
- [18] A.L.W. Sanderson, K. Emoto, J.M. Van Alstine, J.J. Weimer, *J. Colloid Interface Sci.* 207 (1998) 180.
- [19] A. Papra, N. Gadegaard, N.B. Larsen, *Langmuir* 17 (2001) 1457.
- [20] Y.S. Lin, C.-G. Golander, *Colloids Surf. B* 3 (1994) 49.
- [21] G.L. Kenausis, J. Vörös, D.L. Elbert, N. Huang, R. Hofer, L. Ruiz-Taylor, M. Textor, J.A. Hubbell, N.D. Spencer, *J. Phys. Chem. B* 104 (2000) 3298.
- [22] N.-P. Huang, R. Michel, J. Voros, M. Textor, R. Hofer, A. Rossi, D.L. Elbert, J.A. Hubbell, N.D. Spencer, *Langmuir* 17 (2001) 489.
- [23] C. Brink, E. Österberg, K. Holmberg, F. Tiberg, *Colloids Surf.* 66 (1992) 149.
- [24] K. Emoto, J.M. Harris, J.M. Van Alstine, *ACS Symp. Ser.* 680 (1997) 374.
- [25] T.K. Bronich, S.V. Solomatin, A.A. Yaroslavov, A. Eisenberg, V.A. Kabanov, A.V. Kabanov, *Langmuir* 16 (2000) 4877.
- [26] S. Brunner, S. Schuller, R. Kircheis, E. Wagner, *Gene Ther.* 6 (1999) 595.
- [27] P.M. Claesson, E. Blomberg, O. Paulson, M. Malmsten, *Colloids Surf. A* 112 (1996) 131.
- [28] A. Pfau, W. Schrepp, D. Horn, *Langmuir* 15 (1999) 3219.
- [29] G.M. Lindquist, R.A. Stratton, *J. Colloid Interface Sci.* 55 (1976) 45.
- [30] M. Sidorova, T. Golub, K. Musabekov, *Adv. Colloid Interface* 43 (1993) 1.
- [31] A.J. Alpert, F.E. Regnier, *J. Chromatogr.* 185 (1979) 375.
- [32] G. Vanecek, F.E. Regnier, *Anal. Biochem.* 121 (1982) 156.
- [33] P.M. Claesson, O.E.H. Paulson, E. Blomberg, N.L. Burns, *Colloids Surf. A* 123–124 (1997) 341.
- [34] M.-L. Delacour, E. Gailliez, M. Bacquet, M. Morcellet, *J. Appl. Polym. Sci.* 73 (1999) 899.
- [35] E.M. Furst, E.S. Pagac, R.D. Tilton, *Ind. Eng. Chem. Res.* 35 (1996) 1566.
- [36] E.S. Pagac, D.C. Prieve, R.D. Tilton, *Langmuir* 14 (1998) 2333.
- [37] R.D. Tilton, in: R.S. Farinato, P.L. Dubin (Eds.), *Polymer–Colloid Interactions: Techniques and Applications*, Wiley, New York, 1999, p. 331.
- [38] S.B. Velegol, R.D. Tilton, *Langmuir* 17 (2001) 219.
- [39] W.A. Ducker, T.J. Senden, R.M. Pashley, *Langmuir* 8 (1992) 1831.
- [40] S. Biggs, *J. Chem. Soc. Faraday Trans.* 92 (1996) 2783.
- [41] G.J.C. Braithwaite, A. Howe, P.F. Luckham, *Langmuir* 12 (1996) 4224.
- [42] J. Schneider, Y. Dufrêne, W.R. Barger Jr., G.U. Lee, *Biophys. J.* 79 (2000) 1107.
- [43] M. Borkovec, G.J.M. Koper, *Macromolecules* 30 (1997) 2151.
- [44] S. Rex, M. Zuckermann, M. Lafleur, J.R. Silvius, *Biophys. J.* 75 (1998) 2900.
- [45] S. Alexander, *J. Phys.* 38 (1977) 983.
- [46] S. Akari, W. Schrepp, D. Horn, *Ber. Bunsenges. Phys. Chem.* 100 (1996) 1014.
- [47] I.H. Park, E.-J. Choi, *Polymer* 37 (1996) 313.
- [48] D.Y.C. Chan, R.M. Pashley, L.R. White, *J. Colloid Interface Sci.* 77 (1980) 283.
- [49] E. Poptoshev, P.M. Claesson, *Langmuir* 18 (2002) 2590.
- [50] S. Biggs, A.D. Proud, *Langmuir* 13 (1997) 7202.
- [51] P. Linse, *Macromolecules* 29 (1996) 326.
- [52] G.M. Bell, G.C. Peterson, *J. Colloid Interface Sci.* 41 (1972) 542.
- [53] J. Gregory, *J. Colloid Interface Sci.* 55 (1976) 35.
- [54] J. Israelachvili, *Intermolecular and Surface Forces*, Academic Press, New York, 1992, p. 299.
- [55] M.B. Einarson, J.C. Berg, *Langmuir* 8 (1992) 2611.
- [56] P.G. Hartley, P.J. Scales, *Langmuir* 14 (1998) 6948.
- [57] A.C. Hiller, S. Kim, A.J. Bard, *J. Phys. Chem.* 100 (1996) 18808.
- [58] M. Giesbers, J.M. Kleijn, G.J. Fleer, M.A. Cohen Stuart, *Colloids Surf. A* 142 (1998) 343.